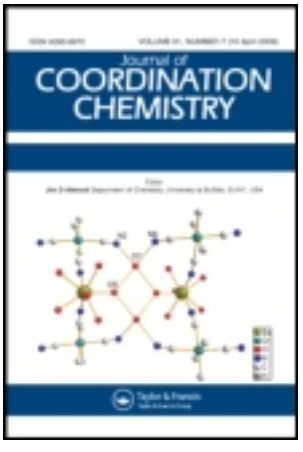

Journal of Coordination Chemistry
Publication details, including instructions for authors and subscription information:
http://www.tandfonline.com/loi/gcoo20

Antibacterial, nuclease, and SOD-mimic behaviors of copper(II) complexes of norfloxacin and phenanthrolines

Mohan Patel [a], Deepen Gandhi [a] & Pradhuman Parmar [a]
[a] Department of Chemistry, Sardar Patel University, Vallabh Vidyanagar - 388 120, Gujarat, India
Published online: 08 Apr 2011.

To cite this article: Mohan Patel, Deepen Gandhi & Pradhuman Parmar (2011) Antibacterial, nuclease, and SOD-mimic behaviors of copper(II) complexes of norfloxacin and phenanthrolines, Journal of Coordination Chemistry, 64:7, 1276-1288

To link to this article: http://dx.doi.org/10.1080/00958972.2011.566922

Journal of Coordination Chemistry
Vol. 64, No. 7, 10 April 2011, 1276–1288

Taylor & Francis
Taylor & Francis Group

Antibacterial, nuclease, and SOD-mimic behaviors of copper(II) complexes of norfloxacin and phenanthrolines

MOHAN PATEL*, DEEPEN GANDHI and PRADHUMAN PARMAR

Department of Chemistry, Sardar Patel University,
Vallabh Vidyanagar – 388 120, Gujarat, India

(*Received 8 October 2010; in final form 1 February 2011*)

Square-pyramidal complexes $[Cu(NFL)(A^n)Cl]\cdot 5H_2O$ (A^n = phenanthroline derivatives and NFL = deprotonated norfloxacin) have been synthesized and characterized. Interactions with Herring Sperm DNA and *pUC19* DNA have been investigated. Mode and extent of interaction was measured by the perturbation in absorbance of complexes in the absence and presence of DNA. Hydrodynamic volume change and gel electrophoretic results were also kept under consideration. Synthesized complexes bind to DNA *via* intercalation with binding constant $0.875–1.446 \times 10^4 (\text{mol L}^{-1})^{-1}$ based on bathochromism and hypochromism observed. Intercalative binding of complexes with DNA was further supported by relative viscosity, where **5** intercalates more strongly with most increase in relative viscosity, and K_b value of $1.446 \times 10^4 (\text{mol L}^{-1})^{-1}$. Evaluation of electrophoretic separation of plasmid on agarose gel reveals that **5** cleaves more efficiently. Square-pyramidal geometry at the metal center supports superoxide-dismutase (SOD)-mimic behavior in addition to an electron-withdrawing group on the ancillary ligand stabilizing Cu–O bonding.

Keywords: Norfloxacin; Antibacterial; Nuclease activity; SOD mimic

1. Introduction

Quinolone is commonly used for a moiety with quinoline-4-one as basic skeleton (figure 1a) [1], whereas fluoroquinolones are synthetic antibacterial agents with fluorine at the sixth and a piperazine ring at the seventh position enhancing antibacterial potency. Norfloxacin is a second generation fluoroquinolone, chemically 1-ethyl-6-fluoro-1,4-dihydro-4-oxo-7-(1-piperazinyl)-quinoline-3-carboxylic acid (NFLH) (figure 1b), an extended spectrum drug for various bacterial infections when administered orally [2], and was patented in 1978.

Many transition-metal complexes are potential probes of nucleic acid structure and are used for potential application as drugs [3]. Copper is a physiologically important element, playing an important role in endogenous oxidative DNA-damage related to aging and cancer. Copper(II) complexes of quinolones and phenanthroline not only bring about oxidative cleavage of DNA but also electrolytic, hydrolytic, and photolytic

*Corresponding author. Email: jeenen@gmail.com

Journal of Coordination Chemistry
ISSN 0095-8972 print/ISSN 1029-0389 online
DOI: 10.1080/00958972.2011.566922

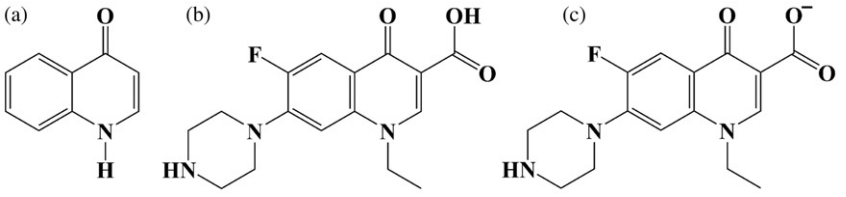

Figure 1. (a) Basic skeleton of quinolones; 4-oxo-1,4-dihydroquinoline. (b) 1-Ethyl(-6-fluoro-1,4-dihydro-4-oxo-7-(1-piperazinyl)-quinoline-3-carboxylic; norfloxacin (NFLH). (c) 1-Ethyl(-6-fluoro-1,4-dihydro-4-oxo-7-(1-piperazinyl)-quinoline-3-carboxylate; deprotonated norfloxacin (NFL).

cleavage [4, 5]. The copper(II) complex of 1,10-phenanthroline can also cleave DNA efficiently [6].

Superoxide radical ($O_2^{\bullet -}$) can cause significant cellular damage. All oxygen-metabolizing organisms possess a metalloenzyme to avoid such harmful effects of superoxide radical, known as superoxide dismutases (SODs). SODs keep the concentration of $O_2^{\bullet -}$ in controlled low limits by disproportionating it to molecular oxygen and hydrogen peroxide [7]. A large number of copper(II) complexes have been found to exhibit such activity [8, 9], which depends on the Cu(II)/Cu(I) redox process, related to flexibility of the geometric transformation at copper [10].

Herein we have studied the structure and biological properties of phenanthrolines–norfloxacin–copper(II) complexes including antimicrobial, DNA-scissoring, and enzymatic activities.

2. Experimental

2.1. *Materials*

Cupric chloride dihydrate (E. Merck), 1,10-phenanthroline, ethidium bromide, bromophenol blue, agarose, Luria broth (LB; Himedia), 2,9-dimethyl-1,10-phenanthroline (**A**[1]), 2,9-dimethyl-4,7-diphenyl-1,10-phenanthroline (**A**[2]), reduced nicotinamide adenine dinucleotide (NADH), nitro blue tetrazolium (NBT), phenazine methosulfate (PMS; Loba chemie), and Herring Sperm DNA (Sigma chemical) were purchased commercially and used as received. Norfloxacin was donated by Bayer AG (Wuppertal).

2.2. *Physical measurements*

Microanalyses (C, H, and N) were done using a 240 Perkin Elmer elemental analyzer. Copper was quantitatively determined from conventional EDTA titration. The d^9 system was confirmed by magnetic moment measurement using Gouy magnetic balance [Mercury(II)tetrathiocyanatocobaltate(II); $\chi_g = 16.44 \times 10^{-6}$ cgs units at 20°C]. Thermograms were recorded on a 5000/2960 SDTA, TA instrument (USA). Electronic spectra were recorded on a UV-160A UV-Vis spectrophotometer, Shimadzu (Japan). Infrared (IR) spectra (4000–400 cm^{-1}) were recorded on a FT-IR Shimadzu spectrophotometer. FAB-mass spectra were recorded on Jeol SX 102/Da–600 mass spectrophotometer/data system using argon/xenon (6 kV, 10 mA) as the FAB gas at an

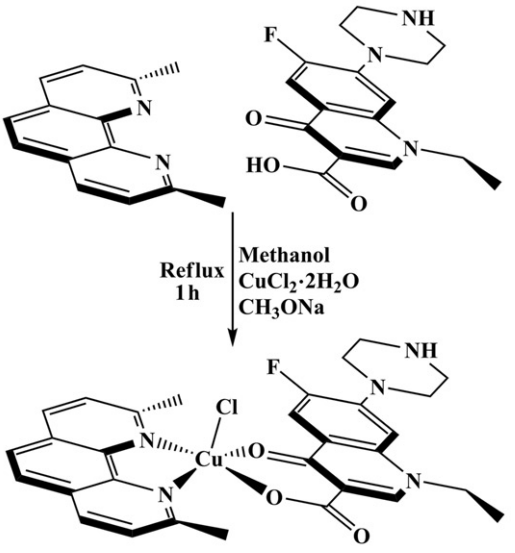

Figure 2. Synthetic scheme of square-pyramidal Cu(II) mixed ligand complexes; reagents and condition: methanolic solutions of $CuCl_2 \cdot 2H_2O$, 2,9-dimethyl-1,10-phenanthroline, norfloxacin (1.5 mmol), NaOMe to transform NFLH to its sodium salt and to adjusted 6.2 pH, 1 h reflux.

accelerating voltage of 10 kV at room temperature. DNA was checked for its protein-free nature by a ratio of UV absorbance (260/280 nm) of 1.8. Photo quantization of the gel after electrophoresis was done using AlphaDigiDoc™ RT Version V.4.0.0 PC–Image software.

2.3. *Synthesis of ligands*

Phenanthroline, 4,5-diazafluoren-9-one ($\mathbf{A^3}$) [11], 1,10-phenanthroline-5,6-dione ($\mathbf{A^4}$) [12], and 5-nitro-1,10-phenanthroline ($\mathbf{A^5}$) [13] were prepared as per reported methods.

2.4. *Synthesis of complexes*

Methanolic solution of $CuCl_2 \cdot 2H_2O$ (1.5 mmol) was added to a methanolic solution of phenanthrolines (A^n) (1.5 mmol), followed by the addition of a previously prepared methanolic solution of norfloxacin (1.5 mmol) in the presence of CH_3ONa (1.5 mmol). The pH of the reaction mixture was adjusted to ~6. The resulting solution was refluxed for 1 h on a steam bath, followed by concentrating to half of its volume. A fine, green amorphous product obtained was washed with ether/hexane and dried in a vacuum desiccator (figure 2).

$[Cu(NFL)(A^1)Cl] \cdot 5H_2O$ (1): It was synthesized by general method using 2,9-dimethyl-1,10-phenanthroline ($\mathbf{A^1}$). Yield: 67.42%; m.p.: 289°C. Anal. Calcd for $C_{30}H_{39}ClCuFN_5O_8$ (%): C, 50.35; H, 5.49; N, 9.79; Cu, 8.88. Found (%): C, 50.20; H, 5.42; N, 9.65; Cu, 8.67. λ_{max}/nm (ε/dm^3 mol^{-1} cm^{-1}), 665 (88). $\mu_{eff.}$: 1.87 BM. m/z: 627 [$C_{30}H_{29}ClCuFN_5O_3 + 3H^+$].

[Cu(NFL)(A^2)Cl]·5H_2O (2): It was synthesized by general method using 2,9-dimethyl-4,7-diphenyl-1,10-phenanthroline ($\mathbf{A^2}$). Yield: 63.32%; m.p.: 264°C. Anal. Calcd for $C_{42}H_{47}ClCuFN_5O_8$ (%): C, 58.13; H, 5.46; N, 8.07; Cu, 7.32. Found (%): C, 58.02; H, 5.51; N, 7.93; Cu, 7.40. λ_{max}/nm (ε/dm^3 mol^{-1} cm^{-1}), 675 (90). $\mu_{eff.}$: 1.78 BM. *m*/*z*: 778 [$C_{42}H_{37}ClCuFN_5O_3 + 2H^+$].

[Cu(NFL)(A^3)Cl]·5H_2O (3): It was synthesized by general method using 4,5-diazafluoren-9-one ($\mathbf{A^3}$). Yield: 58.57%; m.p.: 291°C. Anal. Calcd for $C_{27}H_{33}ClCuFN_5O_9$ (%): C, 47.03; H, 4.82; N, 10.16; Cu, 9.22. Found (%): C, 47.11; H, 4.88; N, 10.01; Cu, 9.11. λ_{max}/nm (ε/dm^3 mol^{-1} cm^{-1}), 672 (83). $\mu_{eff.}$: 1.76 BM. *m*/*z*: 600 [$C_{27}H_{23}ClCuFN_5O_4 + 2H^+$].

[Cu(NFL)(A^4)Cl]·5H_2O (4): It was synthesized by general method using 1,10-phenanthroline-5,6-dione ($\mathbf{A^4}$). Yield: 53.46%; m.p. 278°C. Anal. Calcd for $C_{28}H_{33}ClCuFN_5O_{10}$ (%): C, 46.87; H, 4.64; N, 9.76; Cu, 8.86. Found (%): C, 46.99; H, 4.71; N, 9.60; Cu, 8.77. λ_{max}/nm (ε/dm^3 mol^{-1} cm^{-1}), 684 (85). $\mu_{eff.}$: 1.71 BM. *m*/*z*: 629 [$C_{28}H_{23}ClCuFN_5O_5 + 3H^+$].

[Cu(NFL)(A^5)Cl]·5H_2O (5): It was synthesized by general method using 5-nitro-1,10-phenanthroline ($\mathbf{A^5}$). Yield: 44.45%; m.p. 296°C. Anal. Calcd for $C_{28}H_{34}ClCuFN_6O_{10}$ (%): C, 45.90; H, 4.68; N, 11.47; Cu, 8.67. Found (%): C, 46.01; H, 4.55; N, 11.39; Cu, 8.59. λ_{max}/nm (ε/dm^3 mol^{-1} cm^{-1}), 693 (91). $\mu_{eff.}$: 1.88 BM. *m*/*z*: 642 [$C_{28}H_{24}ClCuFN_6O_5 + H^+$].

2.5. *Antibacterial bioassay* (in vitro)

The complexes were screened for their *in vitro* antibacterial activity against two Gram (+ve) i.e., *Staphylococcus aureus*, *Bacillus subtilis*, and three Gram (−ve) i.e., *Serratia marcescens*, *Pseudomonas aeruginosa*, and *Escherichia coli* species by the broth dilution method by minimum inhibitory concentration (MIC). Two percent of sterile LB was used as a medium which consists of 1% w/v tryptone, 0.5% w/v NaCl, and 0.5% w/v yeast extract. All the cultures were incubated at 37°C. Control tests with no active ingredients and the solvent alone were also performed. Preculture of the bacteria used were grown in LB overnight at an optimal temperature for each species. Bacterial growths were measured by the turbidity of the culture after incubation for 18 h. If a particular concentration of compound inhibits the bacterial growth, half the concentration of the compound was tried. This procedure was continued to a concentration the bacteria grow normally. The lowest concentration that inhibits the bacterial growth was considered as the MIC value. Surroundings were maintained sterile throughout.

2.6. *DNA binding study*

2.6.1. Absorption titration. Perturbation in spectral behavior of the complex on interacting with DNA is a tool for determining the interaction of complexes with DNA. The curves were constructed by increasing the nucleic acid concentration. After adding an equivalent amount of DNA to reference cell, incubation for 10 min at room temperature was provided followed by measurement of absorption. DNA-mediated

hypochromism (decrease in absorbance) or hyperchromism (increase in absorbance) for test compounds was calculated. The results of this assay were generated under the same conditions as the plasmid-degradation assay. This was specifically done to nullify the change in absorbance because of the increasing amount of DNA. From the absorption data, the intrinsic binding constant (K_b) of the complexes with DNA was determined using the following equation:

$$[DNA]/(\varepsilon_a - \varepsilon_f) = [DNA]/(\varepsilon_b - \varepsilon_f) + 1/K_b(\varepsilon_b - \varepsilon_f),$$

where ε_a, ε_f, and ε_b correspond to A_{obsd}/[Complex], the extinction coefficient for free complex, and the extinction coefficient for the complexes in the fully bound form, respectively. A plot of [DNA]/($\varepsilon_a - \varepsilon_f$) *versus* [DNA], where [DNA] is the concentration of DNA in the base pairs, gives K_b as the ratio of slope to *y*-intercept [14].

2.6.2. Viscosity experiments. Change in relative viscosity of DNA in solution was measured by flow-time measurement of solutions containing DNA ($t > 100$ s with error of ± 0.1 s) at 27 ± 0.01°C using a Ubbelohde viscometer and the flow times were corrected for buffer alone (t_0). Flow time for each sample was measured in triplicate and an average time was considered for further calculations. Changes in relative viscosity of DNA for increasing amounts of complexes are represented graphically as $(\eta/\eta_0)^{1/3}$ *versus* concentration ratio of complex to DNA, i.e. [Complex]/[DNA], where η is viscosity of DNA in the presence of complex and η_0 is the viscosity of DNA alone [15]. Viscosity values were calculated using the relation $\eta = t - t_0$.

2.7. *DNA cleavage study*

Gel electrophoresis of plasmid DNA (*pUC19* DNA) was carried out on a 1% agarose gel bed submerged in TAE buffer (0.04 mol L^{-1} Tris-Acetate, pH 8, 0.001 mol L^{-1} EDTA). Fifteen microliters of reaction mixture containing plasmid DNA (150 μg mL^{-1}) in TE buffer (10 mmol L^{-1} Tris, 1 mmol L^{-1} EDTA, pH 8.0) and 200 μmol L^{-1} complex were allowed to proceed for 24 h at 37°C. All the reactions were quenched by the addition of 5 μL loading buffer (40% sucrose, 0.25% bromophenol blue, 0.25% xylene cyanole FF, 200 mmol L^{-1} EDTA). The aliquots were loaded directly onto 1% agarose gel and electrophoresed at 50 V in 1X TAE buffer. Gel was stained with 0.5 μg mL^{-1} of ethidium bromide and was photographed on a UV trans-illuminator. The percentage of each form of DNA was quantified based on illumination using AlphaDigiDoc™ RT Version V.4.0.0 PC–Image software.

2.8. *SOD-like activity*

SOD-like activity of the complexes was determined by using NBT (75 μmol L^{-1}), NADH (79 μmol L^{-1}), and PMS (30 μmol L^{-1}) containing varying concentration of test compounds, that is, 0.25–3.0 μmol L^{-1}. The percentage inhibition of NBT reduction was calculated using the following equation [16]:

$$\text{Percentage inhibition of NBT reduction} = (1 - k'/k) \times 100,$$

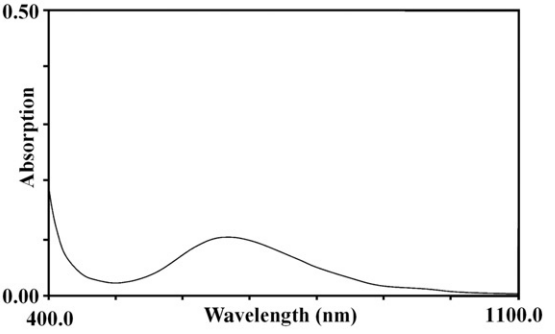

Figure 3. Visible absorption curve for $[Cu(NFL)(A^1)Cl]\cdot 5H_2O$-$d^9$ system exhibiting electronic transition using DMSO as a solvent.

where k' and k are the slope of the straight line of absorbance as a function of time in the presence and absence of a compound, respectively. IC_{50} values of the complexes were determined by linear interpolation from 50% on *Y*-axis onto the *X*-axis on a graph of percentage inhibition of NBT reduction *versus* increasing concentration of the complexes. Concentration of the complexes which causes 50% inhibition of NBT reduction is reported as IC_{50}.

3. Results and discussion

3.1. *Magnetic, electronic, and thermal behaviors*

Magnetic moment measurement generates μ_{eff} of 1.8 μB (Bohr magneton) which is very close to spin-only value for one unpaired electron confirming copper +2 in d^9 configuration ($t_{2g}^6 e_g^3$) [17]. Square-pyramidal geometry at Cu(II) centers show only a broad band ~660 nm in visible electronic transition spectra (figure 3) [18]. In our case λ_{max} about 678 nm in the visible region points toward distorted square-pyramidal geometry. During thermogravimetric analyses, five lattice water molecules were liberated between 60°C and 120°C [19]. Metal content of the complexes was determined from metal oxide at the end of TG curve (>680°C) and are in close proximity to the expected one.

3.2. *IR spectroscopy*

IR spectra of NFLH (table 1) have two strong bands of carboxylate at 1572–1582 cm^{-1} [ν_{asym}(COO)] and 1343–1366 cm^{-1} [ν_{sym}(C=O)]. Unidentate coordination of carboxylate is characterized by $\Delta\nu$ from 215 to 229 cm^{-1} [$\Delta\nu = \nu_{asym}(COO) - \nu_{sym}(COO)$] [20]. Bands at 1625–1632 cm^{-1} in complexes were assigned to ν(C=O), which was appearing at 1730 cm^{-1} for the case of NFLH. The characteristic bands of ν_{asym}(N–H) and ν_{sym}(N–H) of amine remain unchanged on complexation. These data were further supported by ν(M–O) at ~518 cm^{-1} [21]; N→M bonding was supported by ν(M–N) at ~540 cm^{-1} [21].

Table 1. Change in IR bands for interaction of norfloxacin with Cu(II) in addition to phenanthrolines (4000–400 cm^{-1}).

Compounds	ν(C=O) pyridine	ν(H–O) carboxyl	$\nu(COO)_{asym}$	$\nu(COO)_{sym}$	$\Delta\nu$[a]	ν(M–N)	ν(M–O)
NFLH	1730	3350	1642	1336	306	–	–
1	1631	–	1581	1366	215	533	522
2	1625	–	1579	1359	220	538	514
3	1626	–	1582	1355	227	539	528
4	1632	–	1577	1349	228	544	517
5	1630	–	1572	1343	229	547	509

[a]$\Delta\nu = \nu(COO)_{asym} - \nu(COO)_{sym}$.

3.3. *FAB-mass spectroscopy*

From a representative FAB-MS, that is of **1** (figure 4a) and fragments for the same (figure 4b), it can be clearly seen that doublets at 627,629; 553,555; and 306,308 show the isotopic pattern for molecules having one copper and one Cl atom associated with three protons, one proton + matrix, and no proton, respectively. The doublets at 591,593; 563,565; and 381,383 show the isotopic pattern for molecules having one copper. Other peaks for fragments with $m/z = 364$ and 319 are also interpreted from the spectrum. Similar patterns were also observed for the rest of the synthesized complexes.

3.4. *Antibacterial bioassay* (in vitro)

From *in vitro* antibacterial study of $\mathbf{A^1}$–$\mathbf{A^5}$, norfloxacin, and the synthesized complexes (table 2), the ligands have little antibacterial activity compared to NFLH and synthesized complexes but better antibacterial effect than cupric chloride dihydrate. All the synthesized complexes are more potent than drug for all species employed. Data also show that complexes of $\mathbf{A^3}$, $\mathbf{A^4}$, and $\mathbf{A^5}$ are more active than $\mathbf{A^1}$ and $\mathbf{A^2}$. On comparing the obtained data with reported complexes, that is, $[Ni(H\text{-}Ex)_2(H_2O)_2](NO_3)_2$, $[Ag(H\text{-}Ex)_4(NO_3)_2]$ (H-Ex = enoxacin) [22], and $[Cu(HCp)(phen)(H_2O)](OAC)_2 \cdot 4H_2O$ (HCp = ciprofloxacin) [23], although there exist two, four, and one molecule of drug, respectively, for the reported complexes the activity of the complexes synthesized herein are more active, which may be due to the ligands with nitrogen-donor-inhibiting enzyme production [24]. The polarity of metal ion is considerably reduced, which increases lipophilic character favoring metal ion to cross the semi-permeable membrane barrier and interfere in normal cell processes [25]. Other factors that can contribute to the activity are nature of the metal ion, nature of the ligand, coordinating sites and geometry of the complex, concentration, hydrophilicity, lipophilicity, and the presence of CO-ligands.

3.5. *DNA-binding study*

3.5.1. Absorption titration. The changes observed in the absorption curve of the complex after mixing with DNA (either increase/decrease of intensity or shift in λ) indicate that the interaction between complex and DNA takes place directly by

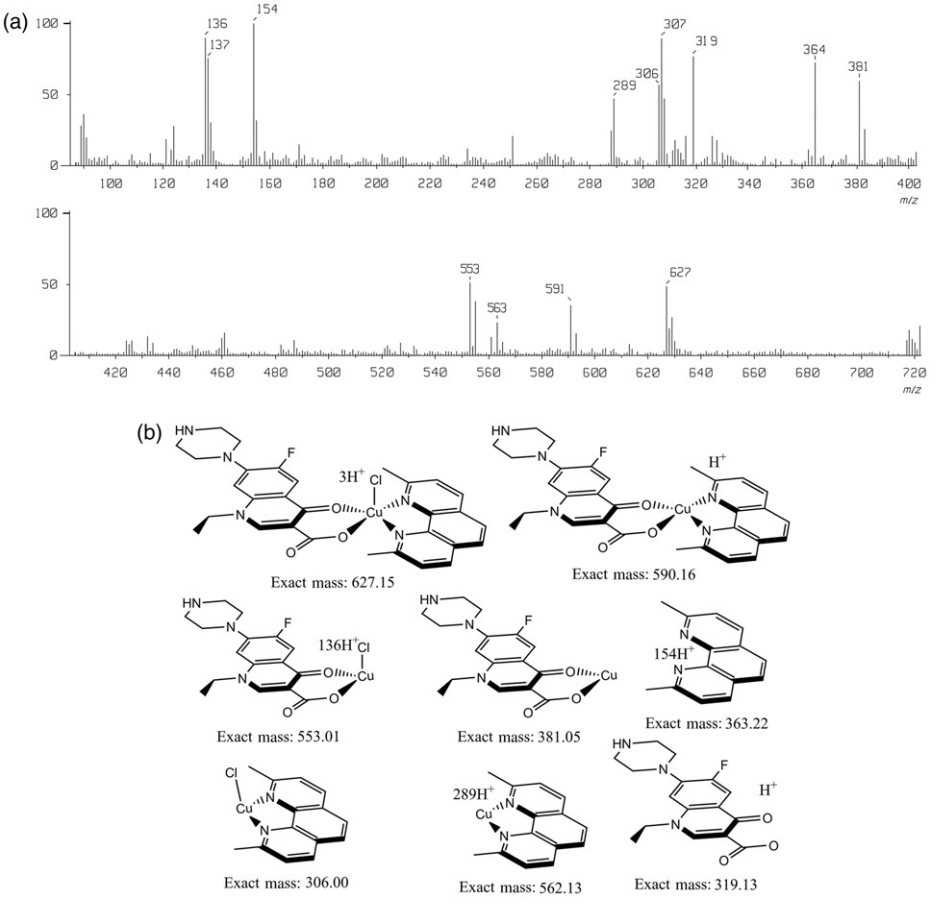

Figure 4. (a) FAB-MS recorded on Jeol SX 102/Da–600 mass spectrophotometer/data system; argon/xenon (6 kV, 10 mA, 10 kV) as FAB gas at room temperature. (b) Proposed fragments of the titled complex corresponding to the peaks observed in its FAB-MS.

Table 2. Bacteriostatic concentration of NFLH, phenanthrolines and their complexes by broth dilution in terms of MIC ($\mu mol\,L^{-1}$).

	Gram positive		Gram negative		
Compounds	*S. aureus*	*B. subtilis*	*S. marcescens*	*P. aeruginosa*	*E. coli*
$CuCl_2 \cdot 2H_2O$	2698.00	2815.00	2756.00	2404.00	3402.00
NFLH	2.50	2.50	4.10	3.80	2.80
A^{1}	130.00	250.00	506.00	154.00	129.00
A^{2}	194.00	169.00	272.00	255.00	278.00
A^{3}	631.00	670.00	604.00	725.00	758.00
A^{4}	829.00	733.00	771.00	738.00	762.00
A^{5}	578.00	631.00	609.00	658.00	591.00
1	2.17	2.28	2.63	2.63	2.35
2	2.33	2.16	3.12	3.40	2.65
3	1.36	1.31	1.09	1.32	1.86
4	1.15	1.52	1.45	1.45	1.54
5	1.32	1.32	1.16	1.20	1.50

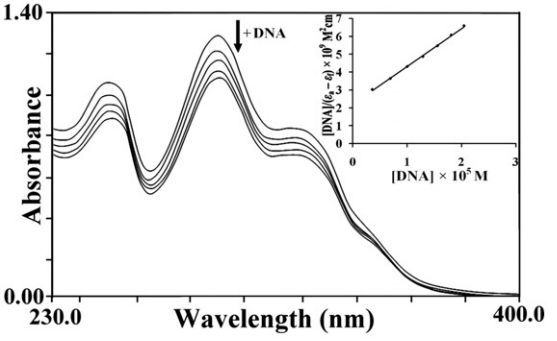

Figure 5. Electronic absorption titration curve to determine binding constant (K_b); recorded for **1** (20 μmol L^{-1}) titrated against increasing concentration of DNA (0–150 μmol L^{-1}) in phosphate buffer (Na_2HPO_4/NaH_2PO_4, pH 7.2) after an incubation period of 20 min at 37°C. Inset: plot of [DNA]/($\varepsilon_a - \varepsilon_f$) *vs.* [DNA].

Table 3. Extent of binding *via* intercalation in terms of binding constant (K_b) and enzymatic behavior to scavenge oxygen radical anion in terms of 50% inhibitory concentration (IC_{50}).

Complexes	K_b (mol L^{-1})$^{-1}$	IC_{50} (μmol L^{-1})
1	0.958×10^4	1.6939
2	0.875×10^4	2.9178
3	1.356×10^4	1.6058
4	1.369×10^4	1.2778
5	1.446×10^4	0.7137

forming a new moiety with double-helix DNA [26]. Intercalation results in hypochromism and a red shift, as this involves a strong stacking interaction between the aromatic chromophore and base pairs of DNA. The magnitude of the hypochromism and red shift are dependent on the strength of intercalation [27]. The spectral curve for diverse complex : DNA mixing ratios (i.e., constant concentration of complex and varying concentration of DNA; figure 5) suggests that the complexes bind to DNA by intercalation; the binding constant values (table 3) suggest **1** and **2** have low binding, attributed to steric constraint of methyl and non-planarity of phenyl ring [28]. The mode of interaction is the same but this difference can be from binding affinity of the synthesized complexes depending on the difference in primary structures of the phenanthroline derivatives employed.

3.5.2. Viscosity measurements. In the absence of crystallographic study, hydrodynamic volume measurement is a most critical test of interaction. Classical intercalation lengthens the DNA helix by base-pair separation, leading to increase in relative viscosity [29]. Binding of classical intercalator ethidium bromide is much greater. Among the synthesized complexes, **5** exhibits large increase in viscosity of DNA compared to the others (figure 6). Increase in DNA viscosity is observed for the complexes but it is quite different from the behavior of $[Ru(phen)_3]^{2+}$ [30], suggesting a classical intercalative mode of binding with DNA [31].

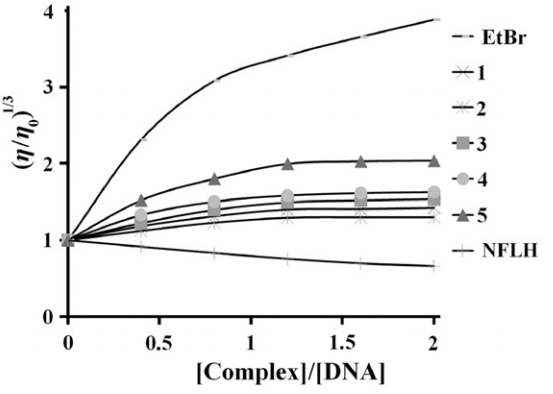

Figure 6. Change in relative viscosity of DNA observed for increasing amount of complexes at $27 \pm 0.1^{\circ}C$ in phosphate buffer (Na_2HPO_4/NaH_2PO_4, pH 7.2).

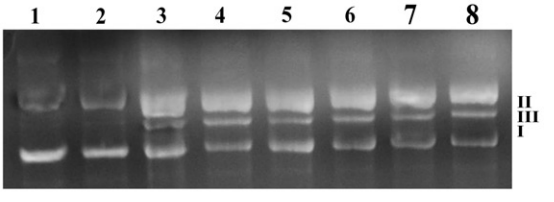

Figure 7. Separation of cleaved *pUC19* DNA ($150\,\mu g\,mL^{-1}$) on interaction with copper(II) complexes ($200\,\mu mol\,L^{-1}$) on 1% agarose gel stained with $0.5\,\mu g\,mL^{-1}$ of ethidium bromide. Interaction between DNA and complexes was allowed for 24 h at 37°C in TE buffer (pH 8) with a final volume of 15 µL; Lane 1, DNA control; Lane 2, $CuCl_2 \cdot 2H_2O$; Lane 3, norfloxacin; Lane 4, $[Cu(NFL)(A^1)Cl] \cdot 5H_2O$; Lane 5, $[Cu(NFL)(A^2)Cl] \cdot 5H_2O$; Lane 6, $[Cu(NFL)(A^3)Cl] \cdot 5H_2O$; Lane 7, $[Cu(NFL)(A^4)Cl] \cdot 5H_2O$; Lane 8, $[Cu(NFL)(A^5)Cl] \cdot 5H_2O$.

Table 4. Plasmid cleavage in terms of relative percentage of all three forms of plasmid separated on 1% agarose gel, at 50V, when $150\,\mu g\,mL^{-1}$ of *pUC19* subjected to different synthesized complexes at $200\,\mu mol\,L^{-1}$ concentration.

Lane No.	Compound	Form I (SC)	Form II (OC)	Form III (LC)
1	Control	81	19	–
2	$CuCl_2 \cdot 2H_2O$	79	21	–
3	Norfloxacin	36	58	6
4	**1**	20	57	23
5	**2**	35	54	11
6	**3**	16	64	20
7	**4**	19	66	15
8	**5**	13	63	24

3.6. *DNA-cleavage study*

For circular plasmid DNA treated with a DNA-scissoring agent when subjected to electrophoresis, the fastest migration is observed for an intact supercoil form (Form I). The open circular (Form II) is the slowest-moving and a linear form (Form III) migrates in between [32]. Data of the cleavage study (figure 7, table 4) show that the

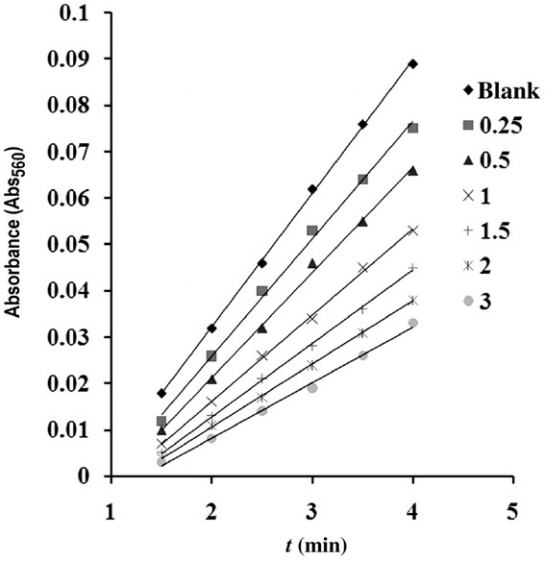

Figure 8. Plot of absorbance (Abs_{560}) as a function of time (t); absorbance corresponding to the amount of formazan formed at varying concentration of **1** (0.25–3 μmol L^{-1}) as function of time.

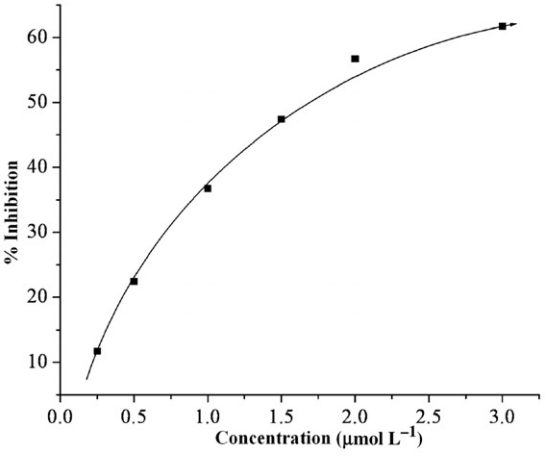

Figure 9. Plot of percentage inhibition of NBT *vs.* increasing concentration of **1** for determining the IC_{50} value.

synthesized complexes are more efficient compared to native NFLH. Among all, **5** is the most efficient. The difference in DNA-cleavage efficiency is because of the difference in the binding affinity of the complexes to DNA due to the difference in the structure of the ancillary ligand.

3.7. *SOD-like activity*

Slopes of the straight line obtained from absorption for mono formazan as a function of time for different concentrations of **1** (figure 8) give the plot for percentage inhibition

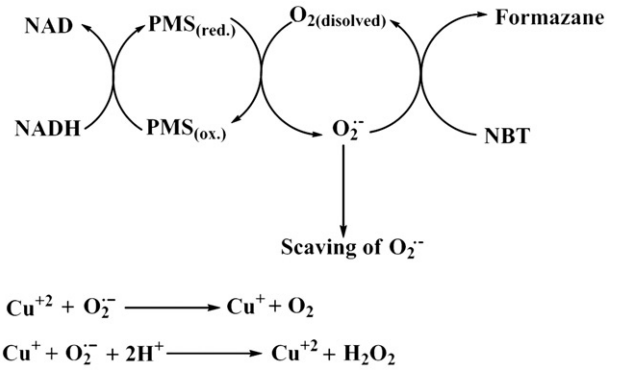

Figure 10. Proposed mechanism for SOD-like activity of complex checked in NBT/NADH/PMS system.

versus concentration (figure 9). SOD-like activity performed at biological pH results in IC_{50} values ranging from 0.7137 to 2.9178 μmol L^{-1} (table 3). The proposed mechanism for generation of ROS and its dismutation is shown in figure 10 [33]. Fee and Huheey proposed rapid interconversion between Cu(II) and Cu(I) *via* electron transfer between copper and reactive oxygen radical anion following the principle of electroneutrality [34].

4. Conclusion

Binding behavior of Cu(II) complexes of phenanthrolines and norfloxacin were subtly but distinctly different depending on the structure of phenanthroline. As the electronegativity of the substituted group on phenanthroline increases, the interaction also increases. The order for interaction of synthesized complexes with DNA from K_b values and change in relative viscosity is **2** < **1** < **3** < **4** < **5**. Ligand which can stabilize bonding between metal center and oxygen radical anion favors enzymatic behavior. In our case, complex with 5-nitro phenanthroline, i.e. complex **5**, showed the highest ability to scavenge free radical anion of molecular oxygen. The synthesized complexes have *in vivo* nuclease, antibacterial, and enzymatic behaviors.

Acknowledgments

The authors thank the Head, Department of Chemistry, Sardar Patel University, India, for making it convenient to work in laboratory and U.G.C. for providing financial support under "UGC Research Fellowship in Science for Meritorious Students" scheme.

References

[1] I. Turel. *Coord. Chem. Rev.*, **232**, 27 (2002).
[2] D.E. King, R. Malone, S.H. Lilley. *Am. Fam. Physician*, **61**, 2741 (2000).
[3] C.J. Burrows, J.G. Muller. *Chem. Rev.*, **98**, 1109 (1998).

[4] C. Tu, Y. Shao, N. Gan, O. Xu, Z. Guo. *Inorg. Chem.*, **43**, 4761 (2004).
[5] P. Ruíz, R. Ortiz, L. Perelló, G. Alzuet, M. González–Álvarez, M. Liu–González, F. Sanz–Ruíz. *J. Inorg. Biochem.*, **101**, 831 (2007).
[6] D.S. Sigman, D.R. Graham, V.D. Aurora, A.M. Stern. *J. Biol. Chem.*, **254**, 12269 (1979).
[7] A.F. Miller. *Curr. Opin. Chem. Biol.*, **8**, 162 (2004).
[8] A.L. Abuhijleh. *J. Inorg. Biochem.*, **68**, 167 (1997).
[9] R.N. Patel, N. Singh, K.K. Shukla, U.K. Chauhan, J. Niclós–Gutiérrez, A. Castiñeiras. *Inorg. Chim. Acta*, **357**, 2469 (2004).
[10] J.C. Casanova, G. Alzuci, J. Borras, J. Latorre, M. Sanau, S. García–Granda. *J. Inorg. Biochem.*, **60**, 219 (1995).
[11] L.J. Henderson Jr, F.R. Fronczek, W.R. Cherry. *J. Am. Chem. Soc.*, **106**, 5876 (1984).
[12] E. Amouyal, A. Homsi, J.C. Chambron, J.P. Sauvage. *J. Chem. Soc., Dalton Trans.*, 1841 (1990).
[13] G.F. Smith, F.Wm. Cagle Jr. *J. Org. Chem.*, **12**, 781 (1947).
[14] A. Wolfe, G.H. Shimer, T. Meehan. *Biochemistry*, **26**, 6392 (1987).
[15] G. Cohen, H. Eisenberg. *Biopolymers*, **8**, 45 (1969).
[16] X. Le, S. Liao, X. Liu, X. Fengz. *J. Coord. Chem.*, **59**, 985 (2006).
[17] M. Melnik. *Coord. Chem. Rev.*, **36**, 1 (1981).
[18] R.N. Patel, N. Singh, K.K. Shukla, V.L.N. Gundla, U.K. Chauhan. *Spectrochim. Acta, Part A*, **63**, 21 (2006).
[19] B.N. Figgis, J. Lewis. In *Principles and Methods*, J. Lewis, R.G. Wilkins (Eds), pp. 400–454, Interscience, New York (1960).
[20] Z.H. Chohan, C.T. Supuran, A. Scozzafava. *J. Enzyme Inhib. Med. Chem.*, **20**, 303 (2005).
[21] H.H. Freedman. *J. Am. Chem. Soc.*, **83**, 2900 (1961).
[22] D.C. Zhong, Z.F. Chen, Y.C. Liu, X.J. Luo, C. Barta, H. Liang. *J. Coord. Chem.*, **63**, 3146 (2010).
[23] Y. Wang, G.W. Lin, J. Hong, L. Li, Y.M. Yang, T. Lu. *J. Coord. Chem.*, **63**, 3662 (2010).
[24] Z.H. Chohan, M. Arif, M.A. Akhtar, C.T. Supuran. *Bioinorg. Chem. Appl.*, **2006**, 13 pp. (2006) doi:10.1155/BCA/2006/83131.
[25] P.K. Panchal, P.B. Pansuriya, M.N. Patel. *J. Enzyme Inhib. Med. Chem.*, **21**, 203 (2006).
[26] G. Psomas, A. Tarushi, E.K. Efthimiadou. *Polyhedron*, **27**, 133 (2008).
[27] J.G. Liu, B.H. Ye, Q.L. Zhang, X.H. Zou, Q.X. Zhen, X. Tian, L.N. Ji. *J. Bioinorg. Chem.*, **5**, 119 (2000).
[28] J.G. Liu, Q.L. Zhang, L.N. Ji. *Transition Met. Chem.*, **26**, 733 (2001).
[29] Q.L. Zhang, J.G. Liu, J.Z. Liu, H. Li, Y. Yang, H. Xu, H. Chao, L.N. Ji. *Inorg. Chim. Acta*, **339**, 34 (2002).
[30] T. Ito, S. Thyagarajan, K.D. Karlin, S.E. Rokita. *Chem. Commun.*, **38**, 4812 (2005).
[31] S. Satyanarayana, J.C. Dabrowiak, J.B. Chaires. *Biochemistry*, **32**, 2573 (1993).
[32] S. Sitlani, E.C. Long, A.M. Pyle, J.K. Barton. *J. Am. Chem. Soc.*, **114**, 2303 (1992).
[33] A.M. Ramadan, M.M. EI-Naggar. *J. Inorg. Biochem.*, **63**, 143 (1996).
[34] J.A. Fee, In *Metal Ions in Biological Systems*, H. Siegel (Ed.) Vol. 13, Marcel Dekker, New York, (1981).